Kinetics-driven anisotropic growth of pentacene thin films

Abdullah Al-Mahboob, Jerzy T. Sadowski, Yasunori Fujikawa, Kazuo Nakajima, and Toshio Sakurai
Institute for Materials Research, Tohoku University, 2-1-1 Katahira, Aoba-ku, Sendai 980-8577, Japan
(Received 23 August 2007; revised manuscript received 9 November 2007; published 22 January 2008)

The growth of nonepitaxial as well as epitaxial structures of (001)-oriented pentacene ($C_{22}H_{14}$, Pn) thin films on silicon surfaces has been extensively studied in order to elucidate the intrinsic thin-film growth mechanism. The kinetically driven growth processes in pentacene films were found to be modified significantly by the anisotropy of the crystal structure. *In situ* real-time low-energy electron microscopy studies of diffusion-limited growth of Pn islands on Si(111)-7×7 and $\alpha\sqrt{3}$-Bi-Si(111) surfaces reveal a definite anisotropy in their shapes. Although this anisotropy is associated with organic film crystal structure, it cannot be predicted directly from the equilibrium crystal shape. It has been found that under kinetic growth conditions the Pn islands are always elongated along the ***b*** axis of the in-plane unit cell, even though the step along the ***a*** axis has the lowest energy, regardless of crystalline polymorph or epitaxial relation, indicating that Pn thin-film growth has an intrinsic kinetic preference along the ***b***-axis direction. Utilizing this kinetic preference and constraining the direction of available flux on inert surfaces during Pn deposition enabled us to control the crystal orientation of Pn domains.

DOI: 10.1103/PhysRevB.77.035426 PACS number(s): 68.55.−a, 68.37.Nq, 68.55.A−, 81.15.−z

INTRODUCTION

Recent progress in the field of organic thin-film transistors (OTFTs)[1–7] receives significant attention underscoring its importance for the microelectronic industry. Among currently investigated organic materials, pentacene (Pn, $C_{22}H_{14}$) appears to be particularly interesting since in terms of field-effect mobility it is comparable to the amorphous silicon devices.[5] The record room temperature (RT) field-effect mobility and hole mobility in organic devices made of single crystal Pn are as high as 5 $cm^2\ V^{-1}\ s^{-1}$ (Mottaghi and Horowitz[7]) and 35 $cm^2\ V^{-1}\ s^{-1}$ (Jurchescu *et al.*[8]), respectively. However, the mobility of Pn thin-film field-effect transistors is at best at the order of ~1 $cm^2\ V^{-1}\ s^{-1}$ (Dimitrakopoulos *et al.*[1] and Jang and Han[6]), which can be explained by the lack of a control over the crystallinity of organic thin films. Organic materials are highly anisotropic, often in both crystal and molecular structures, which complicates their growth mechanisms. Recently, we have observed a highly anisotropic growth of organic, 6,13-pentacenequinone film[9] that was governed by a kinetic growth mechanism related to a structure rather than governed by the thermodynamics. We expect that the kinetic processes in Pn thin-film growth also result in anisotropic islands' evolution. It is to be mentioned that Pn has been found to show strong crystal lattice-related anisotropy in transport properties.[10,11] Therefore, a control of the azimuthal orientation of Pn grains in thin-film fabrication is necessary in order to achieve optimal device performance. This requires also a comprehensive understanding of the kinetic processes controlling the growth of crystalline organic films.

In this work, we studied the kinetic growth anisotropy in Pn thin films by employing low-energy electron microscopy (LEEM). LEEM has an excellent capability of combining the real-time, real-space observations of the film morphology together with the crystallographic analysis by means of microbeam low-energy electron diffraction (μ-LEED). Moreover, use of the low-energy electrons minimizes damage to the specimen, making this technique especially valuable for studying thin organic films. In this paper, we examine growth of Pn on well-characterized silicon surfaces, namely, Si(111)-7×7 and $\alpha\sqrt{3}\times\sqrt{3}$-*R*30 structure of bismuth (Bi) on Si(111) [hereafter, $\alpha\sqrt{3}$-Bi-Si(111)] in order to elucidate the rules governing the kinetics of the pentacene growth. We also demonstrate a possible application of observed kinetic processes to control the azimuthal orientation of organic films by constraining the direction of available molecular flux utilizing one-dimensional surface structures.

EXPERIMENTAL AND CALCULATION PROCEDURES

The growth of Pn thin films on Si(111)-7×7, $\alpha\sqrt{3}$-Bi-Si(111) and Bi(0001)/Si(111) substrates has been studied *in situ* by means of LEEM.[12] Clean Si(111)-7×7 surfaces were prepared by flash heating. The atomically flat $\alpha\sqrt{3}$-Bi-Si(111) substrates[13,14] were prepared by deposition of an equivalent of 1.5 ML (monolayer) of Bi on a Si(111)-7×7 surface, followed by annealing at ~750 K. Annealing removes the excess Bi, leaving exactly 1/3 ML coverage with respect to bulk Si(111) plane. The substrate morphology was verified by scanning tunneling microscopy (STM) in a separate experiment. Bi(0001)/Si(111) substrates were prepared by deposition of ~21 Bi bilayers (BL) of Bi on a clean Si(111)-7×7 surface.[15,16] Self-patterned Bi(0001) surfaces were prepared by depositing a smaller amount of Bi that is required for a complete transition from quasicubic into hexagonal (0001) phase[16] on highly bunched Si(111)-7×7. Pn was thermally evaporated from the tantalum crucible on substrates kept at RT at varying, depending on the experiment, deposition rates of 0.01–0.5 ML/min, where 1 ML corresponds to the molecular density of the Pn(001) plane.[17] Nucleation and growth of Pn films were observed in real time in LEEM, and the μ-LEED patterns were also recorded in the LEEM experiments in order to confirm film crystallinity and to map local crystalline orientations. In the μ-LEED

technique, an aperture placed in the path of electron beam allows one to limit the beam size to approximately 2 μm in diameter on the surface of interest and to choose the probe area, for example, to include both the edge of the Pn island and the bare Si substrate at once. The experimental study of Pn growth was complemented by *ab initio* density functional theory (DFT) calculations using the DFT electronic structure program "Materials Studio Dmol3 Versions 3.1 and 4.0."[18] Geometry optimization for molecular packing was performed in a generalized gradient approximation functional (p91),[19] and subsequent calculations of step energies were done by total electronic energy calculations in the local density approximation functional (pwc).[19(a)] Experimentally obtained unit cell parameters were used as input constraints for the molecular geometry optimization in a two-dimensional Pn lattice. As the real substrate in calculations could not be considered due to limited computing capability, the Pn bilayer with a vacuum slab along a $\langle 001 \rangle^*$ orientation has been constructed, and then optimizations were done for molecular orientations (in-plane, *xy*, coordinates of atoms and relative *xy* coordinates of molecules and molecular tilt) and layer separation (*z*-spacing) between Pn top and bottom layers. This approach allows modeling of a Pn monolayer on an inert surface, with weak bonds between adsorbate and substrate, where the first Pn layer acts as a substrate and the second layer acts as an adlayer. The optimized structures were used for subsequent step energy calculations. Steps were defined by cutting few molecular rows parallel to a low-indexed direction of a vacuum-terminated monolayer supercell parallel to the ***ab*** plane and having the same molecular orientation as in the optimized 2 ML Pn.

RESULTS AND DISCUSSION

Kinetics-driven preferential growth and Pn domain orientations

Thin films of Pn are usually oriented with their (001) crystal planes (also called ***ab*** planes) as the surface planes because the molecular structure and packing anisotropy result in the ***ab*** plane (see Fig. 1) being the most stable crystal face and having much lower energy than other crystal faces.[20] Pn is known to grow nonepitaxially (i.e., without having a relation between the azimuthal orientation of in-plane and substrate lattices), having fractal island shapes on chemically active (having dangling bonds) semiconductor surfaces, such as Si(001)-2×1 (Ref. 21) and Si(111)-7×7 (Ref. 22), after the initial formation of a wetting layer. Meyer zu Heringdorf *et al.*[21] concluded from the analysis of island shapes that in such cases the growth proceeds under the regime of diffusion-limited aggregation (DLA).[23] Our LEEM data confirm that the nucleation of monolayer-high, (001)-oriented Pn islands on the clean Si(111) surface follows the formation of a disordered wetting layer. Random adsorption and possible dissociation of Pn molecules on the Si dangling bonds make the wetting layer very rough [as depicted in the STM image, Fig. 2(a)]. The local roughness of the substrate (interface) reduces the mobility of the molecules, resulting in DLA-like growth of Pn islands. The density of nucleation is rather high—at the flux of 0.5 ML/min, the typical nucleation density is about 3×10^{-2} μm^{-2}. The Pn in-plane lattice parameters obtained from μ-LEED patterns, taken from the second crystalline Pn layer, correspond to a thin-film phase with cell parameters as follows: $|\boldsymbol{a}|=5.71\pm0.07$ Å, $|\boldsymbol{b}|=7.39\pm0.16$ Å, and $\gamma=91.0°\pm0.7°$. The diffraction patterns also indicate rather poor crystallinity of Pn up to the first few layers.

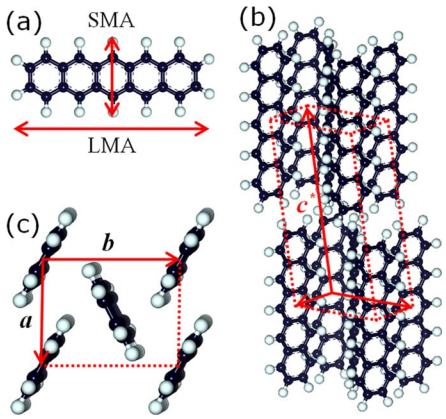

FIG. 1. (Color online) (a) Sketch of a Pn ($C_{22}H_{14}$) molecule; long molecular axis and short molecular axis are shown by arrows. (b) Tilted side view of a Pn unit cell. (c) Molecular packing of Pn in the ***ab*** plane (which is the most stable crystal face) viewed along the direction normal to the surface; the nonequivalent molecule of a herringbone basis is located at $(1/2,1/2)$ with respect to the equivalent molecule at (0,0).

Most interestingly, our real-time LEEM observations of the Pn island evolution on Si(111) reveal a kinetic preference in their development. Mapping of the diffraction patterns into the real space clearly indicates a preferential growth along the ***b*** axis [Figs. 2(b)–2(d)], with anisotropy in an island shape apparent until the diffusion fields of neighboring islands overlap. This preference is in contrast to theoretically predicted surface energies or attachment energies for bulk polymorphs[20,24] and experimental Pn crystal shape.[24] According to these reports, the step energy is lowest for a step parallel to the ***a*** axis and highest for a step parallel to the ***b*** axis; thus, island shapes are not expected to be elongated along the ***b*** axis.

The molecular packing for a Pn thin-film polymorph, with the in-plane lattice parameters derived from μ-LEED data obtained for the Pn film grown on Si(111) via a wetting layer, has been optimized in our DFT calculations; subsequently, the electronic energy of step formation has been calculated. The results of step energy calculations together with experimentally observed growth rate are summarized in Table I. Step energy E_{step} is considered here as the difference between DFT-calculated total energies per step length of the system with and without the presence of the steps. The Wulff plot [Fig. 2(e)] is formed according to the calculated step energies; hence, the equilibrium growth rates perpendicular to the steps can be determined from it.[25] The growth rates derived from Wulff plot as well as experimental growth rates for the Pn monolayer on a Si(111) are also shown in Table I. It is apparent that the Wulff plot of step energies does not reflect the observed anisotropy of the overall island shape. It

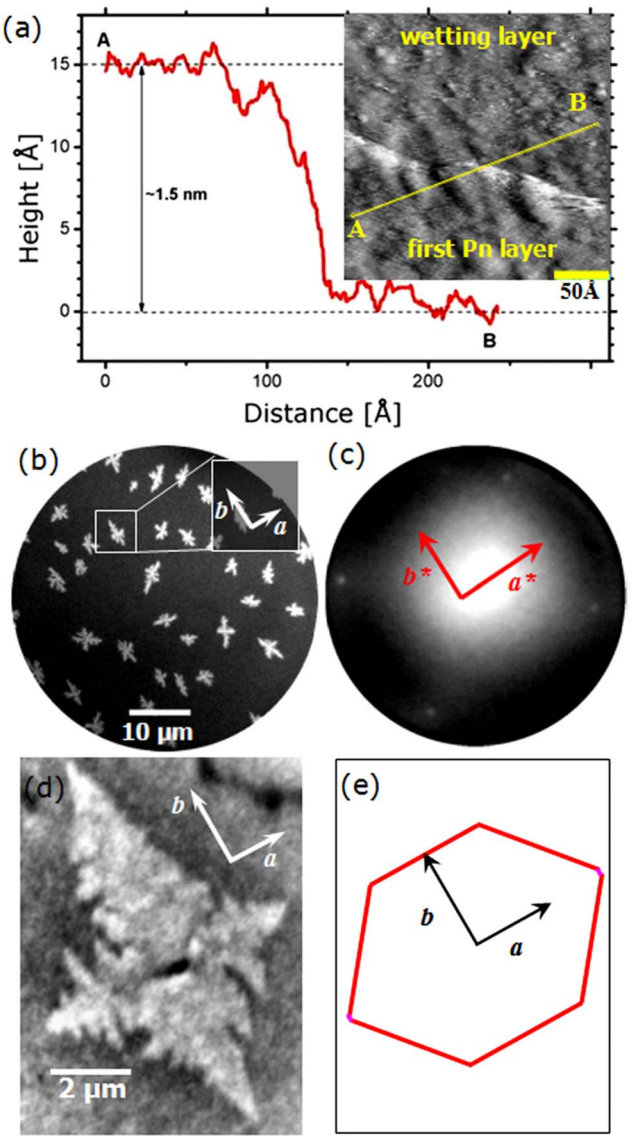

FIG. 2. (Color online) Pn deposited on clean Si(111)-7×7 via a wetting layer: (a) STM image and the line profile taken from the edge of a Pn standing-up monolayer formed on a disordered wetting layer. (b) LEEM image (E=0.2 eV) obtained during Pn deposition on a clean Si(111)-7×7 surface—disordered wetting layer (dark contrast) is formed before the nucleation of a standing-up structure (Pn island, bright contrast); the inset shows the unit cell orientation of the island marked by a rectangle; kinetic preference along the ***b*** axis is observed. (c) μ-LEED pattern (E=10.0 eV) recorded from the second standing-up Pn layer (island) on Si(111); the unit cell orientation of first and second layers are the same. (d) The second layer Pn island at the coverage of 1.2 ML on Si(111); the unit cell orientation is outlined. (e) Wulff plot of calculated electronic step energies of Pn polymorph on Si(111).

is established that the bonding geometry in crystalline structure of elements influences the shape of fractal islands[26,27] governed by a relaxation through the edge diffusion of atoms toward more stable sites. If the growth morphology of Pn is governed by a competition between isotropic fractal growth and equilibrium thermodynamic growth depicted from the Wulff plot, the islands should be elongated along ***a*** axes of the constituent Pn unit cells. However, it is apparent from our LEEM observations that the nonepitaxial islands grown on Si(111) are elongated along the ***b*** axes, regardless of azimuthal orientations of individual islands. It is also to be noted that anisotropies in the growth of first and second crystalline Pn layers are similar. We propose that not only the fractal growth itself, but also the observed overall anisotropy in the evolution of fractal Pn islands is associated with the structure-related kinetics of anisotropic molecule incorporation. We point out that no relaxation or transformation of an island shape are observed upon annealing. If the temperature is raised, Pn molecules desorb from island edges, rather than diffuse along the edge to facilitate a relaxation toward an equilibrium shape. This observation suggests that the kinetic growth-induced shape of Pn island is quite stable, although it is fairly different than its thermodynamic shape.

TABLE I. DFT-calculated step energies of Pn thin-film polymorph grown on Si(111) via wetting layer, and calculated as well as experimental growth rates in this growth system.

Step parallel to	E_{step} (meV/Å)	Growth direction (normal to the step)	Growth rate (relative)	
			Calculated (equilibrium)	Observed (kinetic)
a	90.93	$\boldsymbol{b}^*$	0.74	1
b	122.37	$\boldsymbol{a}^*$	1	0.47 ± 0.07
$\boldsymbol{a}-\boldsymbol{b}$	97.27	$(\boldsymbol{a}+\boldsymbol{b})^*$	0.79	0.28 ± 0.04
$\boldsymbol{a}+\boldsymbol{b}$	98.28	$(\boldsymbol{a}-\boldsymbol{b})^*$	0.80	0.32 ± 0.03

To examine the generality of kinetic preference in thin-film growth, we grew Pn on a flat, chemically inert $\alpha\sqrt{3}$-Bi-Si(111) surface. The corresponding LEEM and μ-LEED data are shown in Figs. 3(a)–3(f). In this case, we observed a very low nucleation density with heterogeneous nucleation usually occurring on defects at the surface. Real-time LEEM observation shows that the nucleation density of the first Pn layer ($<10^{-5}$ μm^{-2}) is 3 orders of magnitude lower than that of Pn on a wetting layer on clean Si(111). LEED patterns taken before the formation of a crystalline Pn layer and taken from the bare substrate near the Pn islands do not show change in the structure of the substrate upon Pn deposition. LEED patterns also show that the film terminates with the (001) surface. These observations imply lack of formation of the wetting layer between standing-up Pn and $\alpha\sqrt{3}$-Bi-Si(111) substrates. The LEED patterns taken from the edge of the Pn island, which contain diffraction spots originated from both substrate surface and Pn layer, show a definite relation between the substrate and Pn film, as shown in Figs. 3(e) and 3(g). The ***b*** axis of the Pn unit cell is rotated by a small angle with respect to one of the three equivalent directions ($\langle 1\bar{1}0\rangle_{Si}$, $\langle 01\bar{1}\rangle_{Si}$, and $\langle \bar{1}01\rangle_{Si}$) of the trigonal substrate surface, such that either the direction $\langle 2\bar{1}\rangle$ or $\langle 21\rangle$ of Pn matches with one of the other directions of these three equivalent substrate surface lattice vectors. The Pn film on $\alpha\sqrt{3}$-Bi-Si(111) has a line-on-line (LOL) coincidence of the film and substrate crystal lattices. Here, the LOL coincidence means that the certain primitive directions (as described above) of the in-plane lattice of Pn match with certain sub-

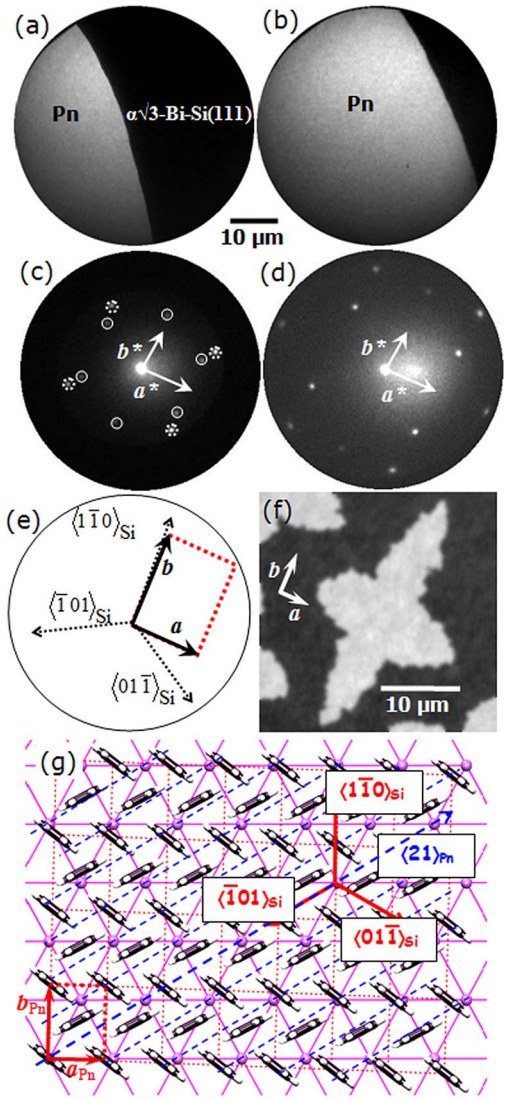

FIG. 3. (Color online) [(a) and (b)] Time-series LEEM images (reflection mode) obtained with a 30 s span during Pn deposition on $\alpha\sqrt{3}$-Bi-Si(111)—a step-flow-like growth of first pentacene layer (bright contrast) having a standing-up structure is observed. Grains are over 100 μm in diameter. (c) μ-LEED pattern (E=8.3 eV) taken from the edge of the Pn island—spots from both substrate (solid circles) and Pn (broken circles) are visible and Pn reciprocal lattice vectors are outlined. (d) μ-LEED pattern (E=17.0 eV) taken from the Pn island; Pn reciprocal lattice vectors are outlined. (e) Sketch of the orientation of the Pn unit cell in relation to the substrate. (f) Bright-field LEEM image (E=1.8 eV) of the second layer island. (g) Adsorption geometry of Pn on an $\alpha\sqrt{3}$-Bi-Si(111) surface showing a line-on-line coincidence between a thin-film polymorph of Pn and the substrate: solid and dotted lines represent the $\sqrt{3}$ superstructure and the Pn lattice, respectively; dashed lines represent the matching direction of lattice lines determined from μ-LEED experiments.

strate surface lattice directions. The Pn in-plane lattice parameters obtained from LEED patterns correspond to the thin-film phase [similar to that in the case of monolayer Pn on Si(111)-(7×7)]: $|\boldsymbol{a}|=5.86\pm0.11$ Å, $|\boldsymbol{b}|=7.34\pm0.17$ Å, and $\gamma=90.6°\pm0.5°$. The formation of a first layer is governed by a step-flow-like growth with a relatively compact (nonfractal) growth front [Figs. 3(a) and 3(b)], and sizes of the grains in the first layer exceed hundreds of micrometers in diameters. The second layer islands have higher densities (typically $\sim0.1\ \mu m^{-2}$). From a combined LEEM/LEED study, it is apparent that the second layer islands are elongated along their ***b*** axes [Fig. 3(f)].

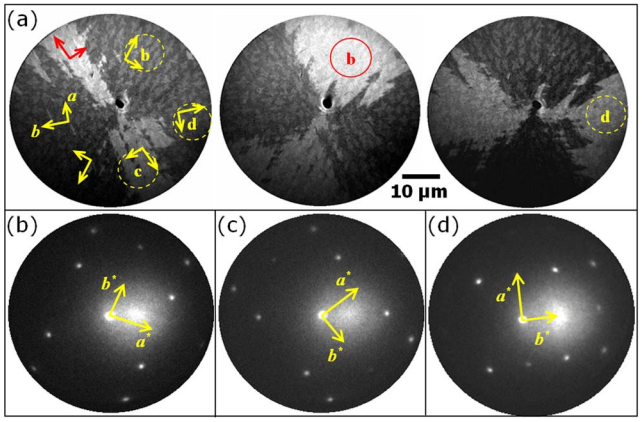

FIG. 4. (Color online) (a) Tilted bright-field LEEM images (E =1.6 eV) of the same area of Pn/$\alpha\sqrt{3}$−Bi-Si(111) under various (arbitrary) tilt conditions of imaging electron beam, showing a bright contrast of particular domains among the trigonally related domains of Pn on $\alpha\sqrt{3}$-Bi-Si(111); second layer islands within the domain are also visible with a weaker contrast; the unit cell orientations depicted from μ-LEED patterns are outlined. [(b), (c), and (d)] μ-LEED patterns taken from the region marked b, c, and d in the images of (a); reciprocal lattice vectors are outlined.

In order to see the kinetic preference in the first Pn layer, after finishing the growth we analyzed the centers of the Pn islands on $\alpha\sqrt{3}$-Bi-Si(111), which happened to nucleate in the vicinity of defects. We could find the region where multiple Pn domains emerged from a single center. Using tilted bright-field imaging, we could obtain contrast between Pn domains having different azimuthal orientations. Figure 4 shows LEEM images of such domains, where six of them nucleated around a substrate's defect [dark spots at the center of images of Fig. 4(a)]. LEED data [Figs. 4(b)–4(d)] indicate that individual domains are epitaxially aligned along three equivalent substrate lattice directions, as described above. The real-space mapping of μ-LEED patterns recorded from each domain evidences that all first layer domains have developed preferentially along the ***b*** axes of their respective in-plane unit cells.

The multiple-domain nucleation is found to be more probable at the substrate defects (heterogeneous nucleation). Such multiple-domain nucleation can evolve also from the initially formed single epitaxial domain because of orientational instability during growth front nucleation, favored by certain epitaxial relations, although the mechanism of this instability is not entirely clear. The domains whose ***b*** axes point toward the available molecular flux grow faster due to kinetic (intrinsic, related to crystal structure) growth anisotropy, suppressing other domains. Recently, we have also reported the LEEM observation of the growth of Pn on H-Si(111). In a Pn/H-Si(111) system, the preferential growth along the ***b*** axis

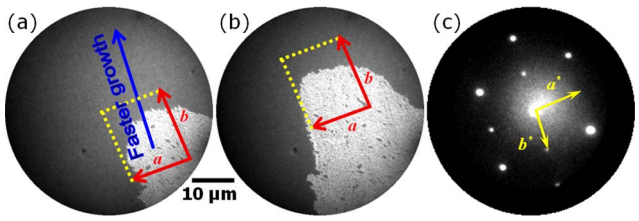

FIG. 5. (Color online) [(a) and (b)] Time-series LEEM images (E=0.7 eV) recorded during Pn deposition at the rate of 0.01 ML/min on Bi(0001)/Si(111) with a time span of 1 min; the images follow the faster growing edge. (c) μ-LEED (10 eV) patterns recorded from the Pn region of images (a) and (b) after stopping deposition; a reciprocal unit cell vector is outlined. In the images, the unit cell vectors depicted from LEED data are outlined, showing that the faster growth is aligned along the ***b*** axis of the corresponding in-plane unit cells.

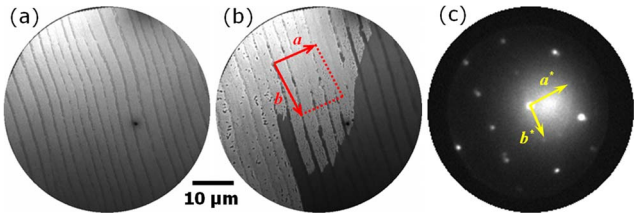

FIG. 6. (Color online) Controlling domain orientation by kinetic constraint: (a) Self-patterned Bi(0001) substrate (bright contrast) separated by the disordered Bi region (dark contrast), which limits Pn molecule's diffusion across it. (b) Pn (bright contrast) on Bi(0001) (gray contrast) having a ***b*** axis closely parallel to the strip direction over the surface within the limit of epitaxial relation. Outlined are the unit cell orientations depicted from μ-LEED; step segments are locally parallel to in-plane diagonals. (c) μ-LEED patterns (E=16 eV) obtained from the Pn island in (b); Pn reciprocal lattice vectors are outlined.

has been also observed,[28,29] underscoring the generality of the observed phenomenon.

In further experiments, the growth of highly ordered epitaxial, bulklike Pn films on the Bi(0001)/Si(111) substrate[22,30] has also been analyzed. It is to be mentioned that Pn/Bi(0001) is the only Pn thin film that has bulklike lattice parameters from the first Pn layer. The growth mode of Pn on annealed Bi(0001)/Si(111) is a step-flow-like growth within the field of view of LEEM, resulting in the formation of a submillimeter Pn domain in the first layer.[22,30] Here, a Pn epitaxial layer is stabilized with a strong point-on-line commensurability between the Pn ***a*** axis and the primitive vectors of the substrate surfacse lattice, in which all Pn molecules are lying on the substrate's surface lattice line along the (01) direction. In order to see the preferential growth directions of Pn on the Bi(0001)/Si(111) surface, the nonannealed surface has been used in this work in order to increase the density of nucleation enhanced by surface roughness. The deposition flux was as low as ~0.01 ML/min in order to decrease the growth rate. After observing the island edge within the field of view of LEEM, the sample position was changed to follow the faster growing edge of the island. Subsequently, the μ-LEED patterns were taken through the domain, following its development. Time-series LEEM images spanned by 1 min, corresponding to faster growing island's edge, are shown in Figs. 5(a) and 5(b). It has been confirmed by real-space mapping of LEED patterns [Fig. 5(c)] that the growth front moves faster in the direction of the ***b*** axis of the corresponding Pn unit cell. The multiple domains that emerged from a single center were also analyzed in LEEM experiments. The μ-LEED data and corresponding real-space mapping show that all the domains are aligned along the ***b*** axes of their respective in-plane unit cells, similar to the cases of Pn grown on other surfaces.

Pn grown on various surfaces in our study correspond to both bulk and thin-film polymorphs and have different commensurations (or no commensuration) with the substrates. Nevertheless, from all the experiments described above, it is clear that Pn grows preferentially along the ***b*** axis, independent of lattice commensuration and the direction of commensuration, when the growth is governed by a kinetics (intrinsic and related to crystal structure). Multiple domains also nucleate at a common center with their ***b*** axes pointing outward, where the incoming molecular flux kinetically assists to orient them, within the limit of epitaxial relations. It is interesting that such multiple-domain nucleation at a single center was not observed in the nonepitaxial DLA growth in the Pn/Si(111)-7×7 system. Further experimental investigations, such as studying the temperature-dependent growth anisotropy with large statistics, as well as accurate theoretical modeling, including more detailed substrate-film interactions, are required to explain the kinetic preference in the growth directions, the relation between epitaxial structures, and the orientational instability.

Controlling domain orientation by constraining flux

Pentacene exhibits anisotropy in electronic transport properties even within a (001) surface plane—the ***ab*** plane.[10,11] Thus, it is important to control the azimuthal orientation of Pn grains in thin-film fabrication in order to achieve optimal thin-film device performance. As discussed above, the Pn domains are oriented with the ***b*** axis aligned outward from a single nucleation center. Orientational instability in growth front nucleation also results in subdomain orientation having the ***b*** axis directed toward available flux within the limit of epitaxial relations. This feature suggests the possibility of controlling domain orientation by constraining flux availability. To check a possibility of controlling azimuthal orientation of Pn in-plane domains by constraining molecular flux on a substrate surface, the self-patterned Bi(0001) surface was prepared by depositing on highly bunched Si(111)-7×7 slightly smaller amount of Bi (<10 BL) than that required for a complete transition from a $(01\bar{1}2)$ orientation to a (0001) orientation.[15] This method allows us to prepare striped region of nearly perfect Bi(0001) structure, separated by a narrow textured $Bi(01\bar{1}2)$ region, as shown in Fig. 6(a). As the $Bi(01\bar{1}2)$ is textured and rough across bunched steps, the mobility of Pn molecules on the $Bi(01\bar{1}2)$ region is lower than that on a flat Bi(0001). Consequently, one-dimensional diffusion of molecules parallel to stripes is achieved. In the

LEEM observation during the growth of Pn on this substrate, it has been found that the steps of growing Pn islands are mostly parallel to in-plane unit cell diagonals within the limit of experimental error. From the combination of LEEM images and LEED patterns, it was clearly found that the films grow preferentially along ***b*** axes of the corresponding in-plane unit cells. The ***b*** axes of Pn islands align only along the directions of Bi(0001) stripes [Figs. 6(b) and 6(c)], i.e., along the direction of unconstrained diffusion of molecules, all giving single crystalline orientation over the observed region of surface. The above observation may have an impact on the practical applications of Pn-based OTFT if one can realize a one-dimensional diffusion of Pn molecules on a dielectric by appropriate patterning of the substrate.

CONCLUSIONS

Experimentally observed growth preference of Pn or overall island shape cannot be predicted from the step energies at equilibrium, nor associated with the competition between DLA and equilibrium growth. The kinetic growth of Pn has a clear preference along the ***b*** axis in the (001) plane, irrespective of the fractal or compact island growth and epitaxial commensuration or nonepitaxial growth. We propose that these preferential growth processes are kinetically related to the anisotropy in the crystal structure and/or molecular structure and bonding (and thus not defined by equilibrium). A detailed modeling of the process requires further investigation. The observed kinetic anisotropy also results in a preference in Pn domain orientations, which tend to have the $\langle 01 \rangle$ direction of the surface lattice aligned with the direction of the available supplied molecular flux. Based on the observation of kinetic preference, by constraining the direction of available flux on an inert flat surface during Pn deposition by constraining the direction of available molecular flux, it may be possible to select a single crystalline orientation, having a ***b*** axis directed along the direction of available flux, within the limit of epitaxial relations, as observed in our experiments.

ACKNOWLEDGMENTS

The authors would like to thank the Center for Computational Materials Science, IMR, Tohoku University for the assistance with the DFT calculations.

[1] C. D. Dimitrakopoulos, S. Purushothaman, J. Kymissis, A. Callegari, and J. M. Shaw, Science **283**, 822 (1999).
[2] A. R. Brown, A. Pomp, C. M. Hart, and D. M. de Leeuw, Science **270**, 972 (1995).
[3] A. Dodabalapur, Z. Bao, A. Makhija, J. G. Laquindanum, V. R. Raju, Y. Feng, H. E. Katz, and J. Rogers, Appl. Phys. Lett. **73**, 142 (1998).
[4] H. Sirringhaus, N. Tessler, and R. H. Friend, Science **280**, 1741 (1998).
[5] C. D. Dimitrakopoulos and P. R. L. Malenfant, Adv. Mater. (Weinheim, Ger.) **14**, 99 (2002).
[6] J. Jang and S. H. Han, Curr. Appl. Phys. **6**, e17 (2006).
[7] M. Mottaghi and G. Horowitz, Org. Electron. **7**, 528 (2006).
[8] O. D. Jurchescu, J. Baas, and T. T. M. Palstra, Appl. Phys. Lett. **84**, 3061 (2004).
[9] A. Al-Mahboob, J. T. Sadowski, T. Nishihara, Y. Fujikawa, Q. K. Xue, K. Nakajima, and T. Sakurai, Surf. Sci. **601**, 1311 (2007).
[10] J. Y. Lee, S. Roth, and Y. W. Park, Appl. Phys. Lett. **88**, 252106 (2006).
[11] G. A. de Wijs, C. C. Mattheus, R. A. de Groot, and T. T. M. Palstra, Synth. Met. **139**, 109 (2003).
[12] E. Bauer, Rep. Prog. Phys. **57**, 895 (1994).
[13] K. J. Wan, T. Guo, W. K. Ford, and J. C. Hermanson, Phys. Rev. B **44**, 3471 (1991).
[14] R. Shioda, A. Kawazu, A. A. Baski, C. F. Quate, and J. Nogami, Phys. Rev. B **48**, 4895 (1993).
[15] T. Nagao, J. T. Sadowski, M. Saito, S. Yaginuma, Y. Fujikawa, T. Kogure, T. Ohno, Y. Hasegawa, S. Hasegawa, and T. Sakurai, Phys. Rev. Lett. **93**, 105501 (2004).
[16] S. Yaginuma, T. Nagao, J. T. Sadowski, A. Pucci, Y. Fujikawa, and T. Sakurai, Surf. Sci. **547**, L877 (2003).
[17] R. B. Campbell, J. M. Robertson, and J. Trotter, Acta Crystallogr. **14**, 705 (1961); R. B. Campbell, J. M. Robertson, and J. Trotter, *ibid.* **15**, 289 (1962).
[18] B. Delley, J. Chem. Phys. **92**, 508 (1990); **113**, 7756 (2000).
[19] (a) J. P. Perdew and Y. Wang, Phys. Rev. B **45**, 13244 (1992); (b) **33**, 8800 (1986); (c) J. P. Perdew, J. A. Chevary, S. H. Vosko, K. A. Jackson, M. R. Pederson, D. J. Singh, and C. Fiolhais, *ibid.* **46**, 6671 (1992).
[20] J. E. Northrup, M. L. Tiago, and S. G. Louie, Phys. Rev. B **66**, 121404(R) (2002).
[21] F.-J. Meyer zu Heringdorf, M. C. Reuter, and R. M. Tromp, Nature (London) **412**, 517 (2001).
[22] A. Al-Mahboob, J. T. Sadowski, T. Nishihara, Y. Fujikawa, Q. K. Xue, K. Nakajima, and T. Sakurai, Surf. Sci. **601**, 1304 (2007).
[23] T. A. Witten, Jr., and L. M. Sander, Phys. Rev. Lett. **47**, 1400 (1981).
[24] L. F. Drummy, P. K. Miska, D. Alberts, N. Lee, and D. C. Martin, J. Phys. Chem. B **110**, 6066 (2006).
[25] M. Wortis, in *Chemistry and Physics of Solid Surfaces VII*, edited by R. Vanselow and R. F. Howe (Springer, Berlin, 1988), p. 367.
[26] Z. Zhang and M. G. Lagally, Science **276**, 377 (1997).
[27] Z. Zhang, X. Chen, and M. G. Lagally, Phys. Rev. Lett. **73**, 1829 (1994).
[28] J. T. Sadowski, G. Sazaki, S. Nishikata, A. Al-Mahboob, Y. Fujikawa, K. Nakajima, R. M. Tromp, and T. Sakurai, Phys. Rev. Lett. **98**, 046104 (2007).
[29] S. Nishikata, G. Sazaki, J. T. Sadowski, A. Al-Mahboob, T. Nishihara, Y. Fujikawa, S. Suto, T. Sakurai, and K. Nakajima, Phys. Rev. B **76**, 165424 (2007).
[30] J. T. Sadowski, T. Nagao, Y. Yaginuma, Y. Fujikawa, A. Al-Mahboob, K. Nakajima, T. Sakurai, G. E. Thayer, and R. M. Tromp, Appl. Phys. Lett. **86**, 073109 (2005).